The Astrophysical Journal, 541:L9–L12, 2000 September 20

STEEPENING OF AFTERGLOW DECAY FOR JETS INTERACTING WITH STRATIFIED MEDIA

Pawan Kumar
Institute for Advanced Study, Princeton, NJ 08540; pk@ias.edu
and
Alin Panaitescu
Department of Astrophysical Sciences, Princeton University, Peyton Hall, Princeton, NJ 08544-1001; adp@astro.princeton.edu
Received 2000 March 15; accepted 2000 August 3; published 2000 September 8

ABSTRACT

We calculate light curves for gamma-ray burst afterglows when material ejected in the explosion is confined to a jet that propagates in a medium with a power-law density profile. The observed light-curve decay steepens by a factor of Γ^2 when an observer sees the edge of the jet. In a uniform density medium, the increase in the power-law index (β) of the light curve as a result of this *edge effect* is ∼0.7 and is completed over one decade in observer time. For a preejected stellar wind ($\rho \propto r^{-2}$), β increases by ∼0.4 over two decades in time as a result of the edge effect, and the steepening of the light curve as a result of the jet sideways expansion takes about four decades in time. Therefore, a break in the light curve for a jet in a wind model is unlikely to be detected even for a very narrow opening angle of a few degrees or less, a case where the lateral expansion occurs at early times when the afterglow is bright.

The light curve for the afterglow of GRB 990510, for which an increase in β of approximately 1.35 was observed on a timescale of 3 days, cannot be explained by only the sideways expansion and the edge effects in a jet in a uniform interstellar medium—the increase in β is too large and too rapid. However, the passage of the cooling or synchrotron peak frequencies through the observing band at about 0.1–1 day together with jet edge effect explains the observed data. The jet opening angle is found to be ∼5°, and the energy in the explosion to be about 10^{51} ergs.

Subject headings: gamma rays: bursts — gamma rays: theory

1. INTRODUCTION

In a recent paper, Chevalier & Li (1999) pointed out that some of the gamma-ray burst (GRB) afterglow light curves are best modeled when the density of the circumburst medium is taken to fall off as r^{-2} (this is referred to as the *wind model*). These afterglows show no evidence for a jet, i.e., their light curves follow a power-law decline without any break. This is puzzling since collimated outflows are expected in the collapsar model for GRBs (MacFadyen, Woosley, & Heger 2000). We offer a possible explanation for this puzzle by showing that the light curve resulting from the interaction of a jet with a pre-ejected wind falls off as a power law whose index changes by an amount smaller than the uniform density interstellar medium (ISM) case and the transition time is much longer.

We carry out a detailed modeling of the multiwavelength afterglow flux data for GRB 990510, which provides the best evidence for a jet propagation in a uniform density medium (Harrison et al. 1999; Stanek et al. 1999), to show that effects associated with a finite jet opening angle alone are insufficient to explain the observed rapid steepening of the light curve. In § 2 we calculate the propagation of a jet in a stratified medium, and in § 3 we describe the calculation of the synchrotron emission and afterglow light curve.

2. DYNAMICS OF EXPANDING JETS

The dynamical evolution of jets and its synchrotron emission have been previously investigated by a number of people (e.g., Rhoads 1999; Panaitescu & Mészáros 1999; Sari, Piran, & Halpern 1999; Moderski, Sikora, & Bulik 2000; Huang, Dai, & Lu 2000). The evolution of the Lorentz factor (Γ) can be calculated from the following simplified set of equations:

$$\frac{dM_1}{dr} = \pi A r^{2-s}\left(\theta^2 + \frac{f\theta}{2\Gamma^2}\right), \tag{1}$$

$$\frac{d\theta}{dr} = \frac{f}{r\Gamma} + \frac{\Theta - \theta}{r}, \tag{2}$$

$$M_0\Gamma + M_1(\Gamma^2 - 1) = M_0\Gamma_0, \tag{3}$$

where θ is the half–opening angle of the jet, M_0 and Γ_0 are the initial mass and Lorentz factor of the ejecta, M_1 is the swept-up mass, $\rho(r) = Ar^{-s}$ is the density of the circumstellar medium, and f (a parameter of order unity) is the ratio of transverse and radial jet velocities; for relativistic outflows, the effect of a constant f on the light curve can be absorbed in Γ_0; Θ is the angle between the velocity vector at the jet edge and the jet axis (in the lab frame) and is determined by the modification of particle trajectory due to the sideways expansion. The second term in equation (1) is due to sweeping up of ISM material resulting from sideways expansion. Equation (3) expresses the conservation of energy, and it applies to an adiabatic shock when the heating of the original baryonic material of rest mass M_0 by the reverse shock is ignored.

The above equations can be combined and rewritten in the following nondimensional form, which is applicable for relativistic as well as nonrelativistic jet dynamics:

$$\frac{dy_1}{dx} = -\frac{x^{2-s}(y_1^2 - \Gamma_0^{-2})^2}{2y_1 - y_1^2 - \Gamma_0^{-2}}\left(y_2^2 + \frac{fy_2}{2\Gamma_0^2\theta_0 y_1^2}\right), \quad (4)$$

$$\frac{dy_2}{dx} = \frac{f}{\theta_0\Gamma_0 x y_1} + \frac{\Theta - \theta}{x\theta_0}, \quad (5)$$

where $x = r/R_{\rm da}$, $y_1 = \Gamma/\Gamma_0$, $y_2 = \theta/\theta_0$, and

$$R_{\rm da} = \left(\frac{E}{\pi A c^2 \theta_0^2 \Gamma_0^2}\right)^{1/(3-s)} \quad (6)$$

is the deacceleration radius, i.e., the radius at which $\Gamma_0/\Gamma \approx 2$; $E = M_0\Gamma_0$ is the energy in the explosion, and θ_0 is the initial half–opening angle of the jet. The above equations show that for the wind and the uniform ISM models $\Gamma \propto t_{\rm obs}^{-1/4}$ and $t_{\rm obs}^{-3/8}$, respectively, as long as $\Gamma \gg \theta_0^{-1}$, where $t_{\rm obs} = \int dt(1 - v)$ is the observer time, t being the lab frame time, and v is the jet velocity in units of c.

Equations (4) and (5) are solved, subject to the boundary conditions $y_1 = y_2 = 1$, for $x \ll 1$. For a relativistic jet with $\Theta = \theta$, i.e., fluid velocity in the radial direction, the solution of equations (4) and (5) depends only on the product $\theta_0\Gamma_0$; in the general case the solution is a two-parameter family of functions. In the relativistic case, ignoring early time behavior, the equation for $y_1 y_2 \equiv y$ is given by

$$\frac{dy}{d\xi} \approx -\frac{y^3}{2} + \frac{1}{\eta\xi}, \quad (7)$$

with $\eta = f(3 - s)(\theta_0\Gamma_0)$, a constant, and $\xi = x^{3-s}/(3 - s)$. An approximate solution to this equation is

$$y \approx \frac{1}{2\xi^{1/2}} + \left(\frac{2}{\eta\xi}\right)^{1/3}. \quad (8)$$

Thus, $y \propto \Gamma\theta$ decreases monotonically with time. The transition to jet sideways expansion starts when the two terms in the above equation become equal, i.e., $\xi \sim (\eta/16)^2$, and lasts for a time interval during which y and Γ decrease by a factor of a few. Therefore, the transition time divided by the time at the start of the transition (in observer frame), during which $\alpha_1 \equiv -d\ln(\Gamma - 1)/d\ln t_{\rm obs}$ increases from $(3 - s)/(8 - 2s)$ to approximately $\frac{1}{2}$, is approximately $9 \times 3^{3/(3-s)}$. The solution to y_1 and y_2 can be obtained by inserting the expression for y into equations (4) and (5). However, y_1 and y_2 determined this way have much larger error than y and should not be used for any serious calculation.

We solve equations (4) and (5) numerically and show the results for $x(t_{\rm obs})$ and $\alpha_1(t_{\rm obs})$ in Figure 1. Note that the change to α_1 from one asymptotic value, corresponding to spherical shell expansion, to another, when sideways expansion is well underway, takes a long time; the ratio of the final to the initial time for a change in α_1 of 0.1 for a uniform ISM is $\sim 10^2$, whereas for $s = 2$ the ratio is 10^3. For the parameters chosen here $\alpha_1 = 0.5$ when Γ is of order a few. In the nonrelativistic phase of the jet expansion $\alpha_1 = 1.2$, as for a Sedov-Taylor spherical shock wave.

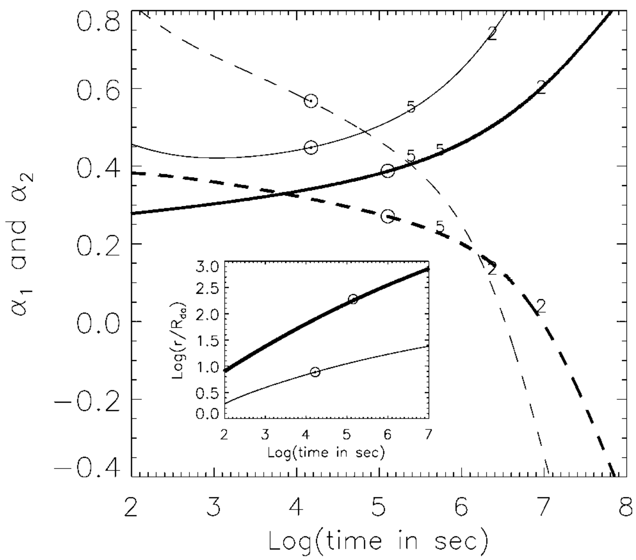

FIG. 1.—$\alpha_1 = -d\ln(\Gamma - 1)/d\ln t_{\rm obs}$ for uniform ISM $s = 0$ (*thin solid curve*) and the wind model $s = 2$ (*thick solid curve*) and $\alpha_2 = -2d\ln(\theta\Gamma)/d\ln t_{\rm obs}$ for $s = 0$ (*thin-dashed curve*) and $s = 2$ (*thick-dashed curve*). The inset shows the evolution of the jet radius. The circled dots mark the time when $\theta\Gamma = 1$, and the numbers denote the time when $\gamma = 5$ (2). For this calculation we took the energy per unit solid angle to be 3×10^{53} ergs sr^{-1} and $\theta_0 = 1/30$ rad. The density of the uniform ISM is 1 cm^{-3}, $A = 5 \times 10^{11}$ g cm^{-1} for $s = 2$, and $\Gamma_0 = 300$ (i.e., $\Gamma_0\theta_0 = 10$).

3. SYNCHROTRON EMISSION FROM RELATIVISTIC JETS

The synchrotron spectrum in the comoving frame is taken to be a sequence of power laws with breaks at the self-absorption, synchrotron peak, and cooling frequencies, as presented in Sari, Piran, & Narayan (1998); these frequencies can be found in, e.g., Panaitescu & Kumar (2000). All of our numerical results, unless otherwise stated, are obtained by integrating emission over equal arrival time surface. Ignoring the radial structure of the jet, the flux received by an observer located on the jet axis is given by

$$f_\nu(t_{\rm obs}) = \frac{1}{8\pi d^2}\int_{r_{\rm min}}^{r_{\rm max}} \frac{P'_{\nu'}(r)}{\gamma^3[1 - v\cos\psi(r, t_{\rm obs})]^2}\frac{dr}{r}, \quad (9)$$

where $P'_{\nu'} = r^3\epsilon'_{\nu'}/(2\gamma)$ is the comoving power per frequency at $\nu' = \gamma(1 - v\cos\psi)\nu$, $r\cos\psi = ct - ct_{\rm obs}$, and $r_{\rm min}$ and $r_{\rm max}$ are solutions of $ct(r_{\rm max}) - r_{\rm max} = ct(r_{\rm min}) - r_{\rm min}\cos\theta(r_{\rm min}) = t_{\rm obs}$.

The observed flux at a frequency that is greater than both the cooling frequency ν_c and the synchrotron peak ν_m is proportional to

$$f_\nu \propto t_{\rm obs}^{(1/2)(4-s)-(1/4)sp}\Gamma^{(1/2)(p+2)(4-s)}\min\{(\theta_0\Gamma_0)^{-2}, y^2\}. \quad (10)$$

At early times when $\Gamma \gg \theta^{-1}$ and $\Gamma \propto t_{\rm obs}^{-(3-s)/(8-2s)}$, the flux decays as $t_{\rm obs}^{-(3p-2)/4}$. At late times when $\Gamma\theta \lesssim 1$, the power-law index for the flux $\beta \equiv -d\ln f_\nu/d\ln t_{\rm obs} = (4 - s)[\alpha_1(p + 2) - 1]/2 + sp/4 + \alpha_2$, where $\alpha_2 \equiv -2d\ln y/d\ln t_{\rm obs}$.

There are two effects that determine the evolution of β. One of them, the *edge effect*, is purely geometrical and results from the angular opening $\sim\Gamma^{-1}$ of the relativistic observing cone becoming larger than the jet opening angle θ, i.e., the observer "sees" the edge of the jet. The increase to β resulting from it is $\alpha_2 \lesssim (3 - s)/(4 - s)$; α_2 decreases with time, and therefore the

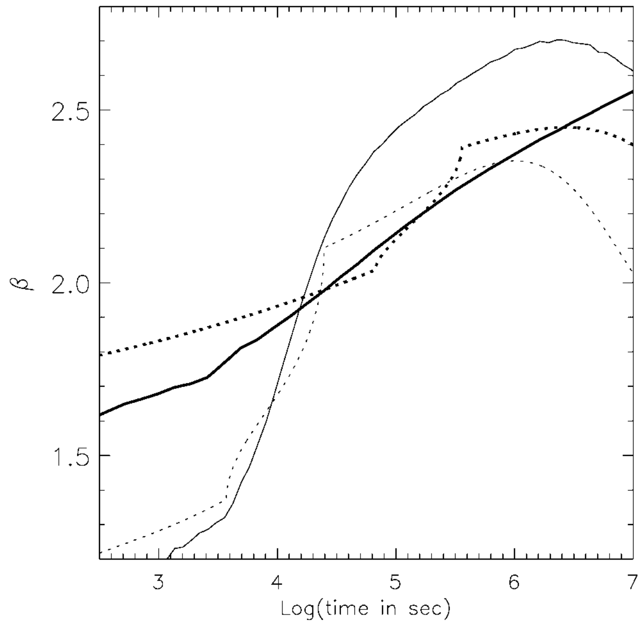

FIG. 2.—$\beta \equiv -d \ln f_\nu / \ln t_{\rm obs}$ for $\nu > \max(\nu_m, \nu_c)$ and $\phi_0 = \theta_0/\sqrt{5}$. The thin- and thick-dashed lines are for $s = 0$ and 2, respectively; the observed flux in these cases was calculated without proper angular integration over the jet surface. The sharp increase to the value of β seen in the dashed curves arises from the edge effect described in the text. The thin and the thick solid curves are for $s = 0$ and 2, respectively, and these calculations included integration over equal arrival time surface; note that this smooths out sharp changes in β. For all of these calculations we took the energy per unit solid angle to be 3×10^{53} ergs sr^{-1}, $\theta_0 = 1/30$ rad ($\theta_0\Gamma_0 = 10$), $p = 2.5$, the density of the uniform ISM equal to 1.0 cm^{-3}, and $A = 5 \times 10^{11}$ g cm^{-1} for $s = 2$. The results shown here are independent of the sideways expansion speed (i.e., the parameter f in eqs. [4] and [5]), as long as this speed is relativistic.

jump in β is smaller for larger θ_0. The dimensionless time for β to increase by α_2 depends on the angular position of the observer with respect to the jet axis and is approximately the ratio of the time when the observer sees the far edge of the jet to the time when the near side of the jet becomes visible; we denote the transition time divided by the time at the onset by R_{t_e}. For an observer located within $\theta_0/2$ of the jet axis, R_{t_e} is 18.7 (81) for $s = 0$ (2), and during this time β increases by approximately 0.7 (0.4). The dependence of R_{t_e} on the angular position of an observer is weak because of integration over equal arrival time surface, which has an effect of smearing the jet edge by an angle $1/\Gamma \sim \theta_0/2$. This sets the minimum value of R_{t_e} to be about 10 (10^2) for uniform (wind) models.

The other effect that leads to a steepening of the afterglow decay is dynamical and is caused by the lateral spreading of the jet. During the relativistic phase the increase to β from the sideways expansion is $\delta\beta = (p + 2)(4 - s)\delta\alpha_1/2 + \delta\alpha_2$; $\delta\alpha_1$ and $\delta\alpha_2$ can be read from Figure 1. Since α_1 does not approach 0.5 asymptotically, $\beta \neq p$ during the relativistic sideways expansion of the jet.[1] The value of β does, however, approach p because $\delta\alpha_1 \approx 1/(8 - 2s)$ sometime before the jet becomes nonrelativistic and $\alpha_2 \approx 0$ at this time, thereby giving $\beta \approx p$ (see eq. [10] and Figs. 1 and 2); β can exceed p, as can be seen in Figure 2.

[1] It should be noted that the asymptotic behavior $\beta \rightarrow p$ for $s = 0$ (Rhoads 1999) is achieved only for extremely narrow jets ($\theta_0 \lesssim 1°$), so that the jet remains relativistic for a sufficiently long time after it starts expanding sideways. It nevertheless serves as a useful, quick way of estimating p approximately from the late time light curve, when β is no longer increasing.

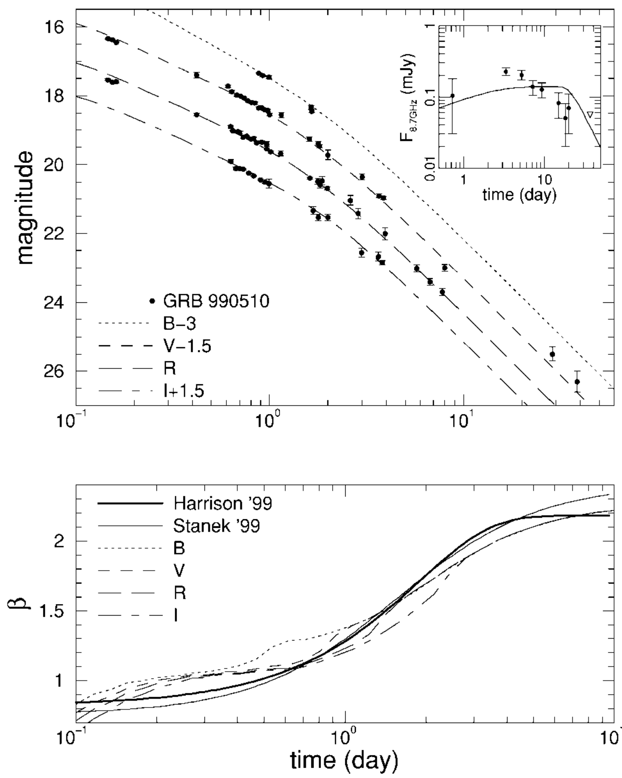

FIG. 3.—Comparison between the observed and the theoretically calculated light curves for the afterglow of GRB 990510 in the radio and the optical bands. Most of the optical data are taken from Harrison et al. (1999) and Stanek et al. (1999). The data sets were supplemented with observations reported by Beuermann et al. (1999), Marconi et al. (1999a, 1999b), and Pietrzynski & Udalski (1999a, 1999b). The *B*-band magnitudes are only from Stanek et al. (1999). The two latest *V*-band magnitudes were measured with the *HST* (Fruchter et al. 1999). The inset of the upper panel shows the 8.7 GHz emission (data were taken from Harrison et al. 1999). The model light curves are calculated for an observer located on the jet axis, which gives the fastest decline of the light curve. The jet has energy per solid angle $E/(\pi\theta_0^2) = 1.2 \times 10^{54}/4\pi$ ergs sr^{-1} and a half-angle $\theta_0 = 0.04$ rad. The electrons acquire $\epsilon_e = 0.3$ of the internal energy after shock acceleration, the magnetic field energy is $\epsilon_B = 0.001$ of that of the shocked gas, and the electron index is $p = 2.2$. The external medium is homogeneous with $n = 0.23$ cm^{-3}. The redshift of the source is $z = 1.62$. The cooling frequency passes through the observing window at $t_{\rm obs} = 1.2$ days, steepening the afterglow light curve while the sideways expansion is effective. The lower panel shows a comparison of the numerically computed power-law index (β) for the decline of the afterglow of GRB 990510 and the observed one, as obtained by the fitting formula given in Harrison et al. (1999) and Stanek et al. (1999).

However, the decrease in α_2 during the mildly relativistic phase prevents β from getting much larger than p. This result can be extended to any observing frequency $\nu > \nu_m$ after an appropriate modification of equation (10). For instance, to consider the case of $\nu_c > \nu > \nu_m$ the right-hand side of the equation should be multiplied by a factor of $(t_{\rm obs}\Gamma^2)^{(1-3s/4)}$, which has little effect on the evolution of β. The timescale for the increase in β due to sideways expansion is of order 10^2 (10^3) for $s = 0$ (2) (see Fig. 2). Therefore, this effect is smaller than that resulting from seeing the jet edge, and it extends over a much longer time.

To conclude, we wish to emphasize that for most jets propagating in a uniform ISM we are likely to see an increase to β of only 0.6–0.9; the remainder of the increase takes place on a long timescale and thus is hard to detect. For jets in a *windy medium*, $s = 2$, β changes by less than about 0.5 and the transition time $R_{t_e} \sim 10^3$. Such a gradual increase to the afterglow light curve power-law index is extremely difficult to detect (see Fig. 2). For instance, if the edge of the jet becomes visible at $t_{obs} \sim 1$ day, the difference in the optical flux at the end of 10 days with and without a jet is ~0.25 mag, which can be easily missed. Thus, the GRBs studied by Chevalier & Li (1999), which show evidence for the wind model, could in fact have had a highly collimated ejection of material.

3.1. *The Afterglow of GRB 990510*

The optical emission of the afterglow of GRB 990510 was measured in the *V*, *R*, and *I* bands between 0.15 and 7 days after the burst and showed the power-law index of the light curve β to have increased from 0.82 ± 0.02 to 2.18 ± 0.05 (Harrison et al. 1999) or from 0.76 ± 0.01 to 2.40 ± 0.02 (Stanek et al. 1999) during a dimensionless time $R_{t_e} \approx 30$, which, as described previously, is not possible to obtain through the effects of the jet sideways expansion alone. There should be some contribution to the light-curve steepening due to the passage of one (or both) of the spectral breaks: the synchrotron peak ν_m and the cooling frequency ν_c.

In Figure 3 we show a comparison between the light curves of GRB 990510 in the *V*, *R*, and *I* bands and the 8.7 GHz radio data with a model of a jet in a uniform ISM where the cooling frequency ν_c crosses the optical band at $t_{obs} \sim 1$ day; we solve equations (4) and (5) and use equation (9) to calculate the theoretical light curves. The steepening of the light curve has little dependence on the observing band because the ratio of the largest to the smallest optical wavelength is ~1.5. Moreover, the integration over angle spreads in time the steepening of β, making it nearly achromatic. An increase of β by ~0.8 is caused by the jet edge and the sideways expansion, and an increase of 0.25 results from the passage of ν_c through the observing band. A further increase of β of ~0.15 is caused by the passage of ν_m through the observing band at $t_{obs} \sim 0.03$ days (see lower panel of Fig. 3); the transition time for β to increase by $\sim(3p - 1)/4$ due to the ν_m crossing is about a decade in the observer frame as a result of integration over equal arrival time surface; hence, one should be careful in deducing p from β at early times. All these together give rise to a light curve that is consistent with the data. The model is also consistent with the *Hubble Space Telescope* (*HST*) *V*-band observation carried out about a month after the burst (Fruchter et al. 1999). Moreover, since ν_c crosses the X-ray band at a few seconds we expect the break in the X-ray light curve to be smaller than optical by ~0.25, which is consistent with observations (Kuulkers et al. 2000). The parameters for the fit are given in the caption for Figure 3, which yields the energy in the burst to be 5×10^{50} ergs. Correcting for the radiative losses, the energy in the burst increases by a factor of a few to $\sim 10^{51}$ ergs. We estimate the uncertainty in model parameters by varying them in such a way that the numerically calculated light curve lies within 3 σ of the observed data points. We find the uncertainty in the jet opening angle and the burst energy to be a factor of 2 and 5, respectively, and ϵ_e, n, and ϵ_B are found to be uncertain by factors of about 4, 40, and 7, respectively; we note that the radio observations are very important in constraining the model parameters. The electron index p is constrained by the observed β before and after the ~1 day break; the error in p is ~5%.

The optical emission of the afterglow of GRB 990510 can also be explained by a model where the synchrotron peak frequency crosses the observed band at ~0.1 days. Its effect on β persists for up to ~1 day and yields an increase of β of ~0.5 during the early observations.

4. CONCLUSIONS

One of the main results of this work is to show that afterglows from even highly collimated GRB remnants going off in a medium with density decreasing as r^{-2} show little evidence for light-curve steepening when $\Gamma\theta \sim 1$. This could explain the lack of breaks in the afterglows of GRB 980326 and GRB 980519, which Chevalier & Li (1999) found to offer support for the wind model. Jets can perhaps be detected by the measurement of time-dependent polarization.

In a collimated outflow the sharpest break in the light curve is produced in a uniform density circumstellar medium and is associated with the edge of the jet coming within the relativistic beaming cone (the edge effect). The magnitude of this break is ~0.7 (0.4) for a uniform ISM (wind model), and 90% of the steepening is completed over about 1 decade (2 decades) in time. Further steepening of the light curve, associated with the sideways expansion of the jet, occurs on a much longer dimensionless timescale of $R_{t_e} \sim 10^2$ (10^4), i.e., weeks to months.

The power-law index for the light curve of GRB 990510 increased between days 0.8 and 3 by about 1.35. This is too large and too fast to result from jet edge and sideways expansion effects. However, the observations can be explained if either the cooling or the synchrotron peak frequency passed through the observing band at about 1 or 0.1 days, respectively. Models that are consistent with both the optical and radio data of this afterglow have an opening angle of ~5°, and energy in the explosion is about 10^{51} ergs (see Fig. 3).

For the afterglow of GRB 990123 the power-law index of the light curve increased by 0.55 between days 1.5 and 3, which can be explained by the edge effect alone (Mészáros & Rees 1999).

We thank Peter Mészáros and Vahe Petrosian for useful discussions and Tsvi Piran for helpful comments on the Letter.

REFERENCES

Beuermann, K., Reinsch, K., & Hessman, F. 1999, GCN Circ. 331 (http://gcn.gsfc.nasa.gov/gcn/gcn3/331.gcn3)
Chevalier, R. A., & Li, Z.-Y. 1999, ApJ, 520, L29
Fruchter, A., et al. 1999, GCN Circ. 386 (http://gcn.gsfc.nasa.gov/gcn/gcn3/386.gcn3)
Harrison, F., et al. 1999, ApJ, 523, L121
Huang, Y., Dai, Z., & Lu, T. 2000, A&A, submitted (astro-ph/0002433)
Kuulkers, E., et al. 2000, preprint (astro-ph/0003258)
MacFadyen, A., Woosley, S. E., & Heger, A. 2000, ApJ, submitted (astro-ph/9910034)
Marconi, G., et al. 1999a, GCN Circ. 329 (http://gcn.gsfc.nasa.gov/gcn/gcn3/329.gcn3)
Marconi, G., et al. 1999b, GCN Circ. 332 (http://gcn.gsfc.nasa.gov/gcn/gcn3/332.gcn3)
Mészáros, P., & Rees, M. J. 1999, MNRAS, 306, L39
Moderski, R., Sikora, M., & Bulik, T. 2000, ApJ, 529, 151
Panaitescu, A., & Kumar, P. 2000, ApJ, in press (astro-ph/0003246)
Panaitescu, A., & Mészáros, P. 1999, ApJ, 526, 707
Pietrzynski, G., & Udalski, A. 1999a, GCN Circ. 319 (http://gcn.gsfc.nasa.gov/gcn/gcn3/319.gcn3)
———. 1999b, GCN Circ. 328 (http://gcn.gsfc.nasa.gov/gcn/gcn3/328.gcn3)
Rhoads, J. 1999, ApJ, 525, 737
Sari, R., Piran, T., & Halpern, J. 1999, ApJ, 519, L17
Sari, R., Piran, T., & Narayan, R. 1998, ApJ, 497, L17
Stanek, K., Garnavich, P., Kaluzny, J., Pych, W., & Thompson, I. 1999, ApJ, 522, L39